Synthesis and optical properties of SiO_2–Al_2O_3–MgO–K_2CO_3–CaO–MgF_2–La_2O_3 glasses

C R GAUTAM[#]

Advanced Glass and Glass Ceramic Research Laboratory, Department of Physics, University of Lucknow, Lucknow 226007, India
[#]Present address: Department of Materials Science and Nano Engineering, Rice University, P.O. Box 1892, Houston, Texas 77005, USA

Abstract. A series of five glass compositions were prepared by using the conventional melt quenching technique in the system SiO_2–Al_2O_3–MgO–K_2CO_3–CaO–MgF_2–La_2O_3 with different contents of SiO_2, MgO, K_2CO_3, MgF_2 and La_2O_3. The effects on the optical and physical properties of these glasses due to the addition of La_2O_3 as well as variation of the various oxides have been investigated. X-ray diffraction analysis is used to confirm the amorphous nature of the prepared glasses. Structures of glasses were studied by using UV–Vis and Fourier transforms infrared spectroscopy. The drilling test was also performed on their glass ceramic samples to confirm the machinability.

Keywords. Glasses; XRD; FT-IR; UV–Vis spectroscopy; machinability.

1. Introduction

The fundamental building block is SiO_4 tetrahedral unit, and in pure SiO_2, all the oxygens are shared between two tetrahedra forming a fully polymerized network. Alkali or alkaline earth cations act as network modifiers, breaking bridging oxygen bonds to form non-bridging oxygens (NBOs) and residing in sites interstitial to the tetrahedral network in the vicinity of the negatively charged NBOs [1]. In 1970, Beal *et al* [2] reported machinable glass–ceramics containing phlogopite from the SiO_2–B_2O_3–MgO–Al_2O_3–K_2O–F glass system. Grossman [3] obtained tetrasilicic–mica glass–ceramics from the K_2O–MgF_2–MgO–SiO_2 glass system. The structure of phlogopite is composed of a two-dimensional network of corner-shared $[SiO_4]^-$ and $[AlO_4]^-$ tetrahedra, forming an hexagonal ring. A layer of Mg^{2+} ions in octahedral coordination is located between two tetrahedral layers [4]. The triple layers are connected to each other by relatively large alkali ions, e.g., K^+ or Na^+. Few systematic studies may be found on the influence of glass compositions on the formation of fluorphlogopite crystal phase [5]. Mg^{2+} is an important component of the mica structure, so MgO content affect the glass structure and the formation or shape of mica crystals [6]. Glass properties may be explained on the basis of network connectivity (NC), which is the number of bridging oxygen atoms (BO) per network forming element [7]. Thus, pure silica glass has an NC of 4 while a glass structure consisting of linear $[SiO_3]_n^{2n-}$ chains has an NC of 2. NC can be used to predict glass surface reactivity, solubility or the likelihood of undergoing glass-in-glass phase separation and bioactivity [8].

Recently, a lot of work has been reported on the doping of different concentrations of La_2O_3 for $(Pb,Sr)TiO_3$/$(Ba,Sr)TiO_3$ borosilicate glasses to act as network modifiers as well as nucleating agents [9–11]. Ceramic base materials are not suitable for some applications because of their brittle properties with respect to mechanical effects, such as cutting and drilling [12]. However, some modifications in chemical composition and production methods can provide better mechanical behaviour. One of the important materials that can be used to improve the machinability of ceramics is mica-based glass ceramics. Mica-based glass ceramics are used as high quality electrical insulators and exhibit high resistance to thermal shock and good machinability [13]. Mica-based glass ceramics based on the SiO_2-MgO-MgF_2-K_2O system are commercially produced and exhibit unique properties, such as remarkable cleavage, flexibility and elasticity, enabling excellent machinability [14]. Commercial mica-based glass ceramics are primarily of the fluorophlogopite type [15]. The glass ceramic derived from this investigated glass SiO_2–Al_2O_3–MgO–K_2CO_3–CaO–MgF_2–La_2O_3 system are technologically very useful for machinable glass ceramics which have very important device applications such as crown, artificial bone, etc. More recently, a nominal composition of SiO_2 40%, Al_2O_3 12%, MgO 10%, MgF_2 24%, CaO 5%, K_2O 1% and ZrO_2 8% in weight ratio has been reported for dental CAD/CAM system [16].

In this research paper, our aim is to explore the structural networking between different glasses as formed and compositional effect due to variation of La_2O_3 on optical properties of the glass system SiO_2–Al_2O_3–MgO–K_2CO_3–CaO–MgF_2–La_2O_3, because such type of results are not reported

---

gautam_ceramic@yahoo.com

so far. The optical characterizations give the valuable information about the formation of bonding network between different oxide groups and crystallization. Hence, their glass ceramic can be easily machined for different device applications.

2. Experimental

2.1 *Glass sample preparation*

Five different glass compositions according to table 1 in the SiO_2–Al_2O_3–MgO–K_2CO_3–CaO–MgF_2–La_2O_3 glass system has been synthesized from high purity ($\geq 99\%$) raw materials: SiO_2, Al_2O_3, MgO, K_2CO_3, CaO, MgF_2 and La_2O_3. Appropriate amounts of chemicals were weighed by using a digital balance with an accuracy of 0.0001 g. The weighed chemicals were thoroughly mixed in an agate mortar and pestle in acetone media until they were dried. The dried powders were melted in high pure alumina crucible at 1350–1450°C for 1 h until a bubbled free liquid was formed using electric furnace. The glass melt has been cast onto an aluminium block and quickly transferred into a preheated muffle furnace for annealing at 475°C for 3 h to avoid breaking of the glass samples through residual internal strain and then furnace cooled to room temperature. The prepared glass block was cut into small pieces for further characterizations.

2.2 *X-ray diffraction*

Glass samples have been grinded with the help of mortar pestle to obtain fine powder. X-ray diffraction (XRD) data of powdered glass samples was recorded by a Rigaku Miniflex-II X-ray diffractometer using CuKα radiation with step size of 0.02° over the 2θ range of 10–80°.

2.3 *Density measurements*

Density of the glass samples depend upon the variation of La_2O_3 as well as on compositional changes. Therefore, the density of the prepared glass samples has been calculated by using Archimedes Principle [17]. Distilled water was used as the liquid medium. The densities of these glass samples are listed in table 1. The following formula was used for determination of density of the glass samples.

$$\text{Density} = \frac{(W_2 - W_1)}{(W_4 - W_1) - (W_3 - W_2)}, \tag{1}$$

where W_1 is the weight of empty specific gravity bottle (in grams); W_2 the weight of specific gravity bottle with sample (in grams); W_3 the weight of specific gravity of bottle with sample and distilled water (in grams); W_4 the weight of specific gravity bottle with distilled water (in grams). Density of distilled water is 1.0 g cm^{-3}.

2.4 *Fourier transform infrared spectroscopy*

Fourier transform infrared absorption spectra of the annealed glasses were obtained at room temperature in the wavenumber range of 4000–400 cm^{-1} using a Fourier transform infrared spectrometer ((FT-IR), BX-II, Perkin Elemer). The samples were grinded into fine powder ($<$180 μm) and then mixed with KBr powder in the ratio of 1:9 precisely. Subsequently, the mixtures were uniaxially pressed to form clear homogeneous discs. The FT-IR measurements were carried out immediately after preparing the discs to avoid moisture absorption. Chemical bonds in different environments will absorb varying intensities and at varying frequencies.

Table 1. Various glass compositions melted in mol percentage of oxides, density, optical band gap, type of vibrations and peak position in the FT-IR spectra of G1, G2, G3, G4 and G5 glass samples.

Glass code	Oxide (mol%)							Density (g cc^{-1})	Optical band gap (eV)	No. of peaks	Peak position (cm^{-1})	Assignments	Wavenumber of different absorption peaks (cm^{-1})			
	SiO_2	Al_2O_3	MgO	K_2CO_3	CaO	MgF_2	La_2O_3						1	2	3	4
G1	48	12	16	8	6	5	5	3.298	3.59	1	1631	Si–OH, OH (molecular water)	1631	1384	759	645
G2	42	12	14	8	6	14	4	3.068	3.63	2	1384	Hydrogen bonding	1630	1383	761	638
G3	40	12	12	10	6	17	3	3.031	3.65	3	759–777	Stretching vibration of SiO_4 tetrahedron	1630	1383	777	639
G4	38	12	10	12	6	20	2	2.277	3.65	4	670–704	Bending vibrations of Si–O–Si and Si–O–Al linkages	1631	1383	766	642
G5	36	12	8	14	6	24	0	2.104	3.63	5	645–615	Asymmetric stretching vibrations of Al–O–Al bond of octahedral (AlO_6) units	1631	1384	759	644

2.5 *UV–Vis spectroscopy*

UV–visible absorption spectroscopy is a very useful technique to characterize the optical and electronic properties of different materials such as thin films, filters, pigments and glasses. Measurement of the optical band gap of glass samples is carried out using the data within the wavelength range from 300–900 nm obtained by spectrophotometer. UV–Vis spectroscopy of the glass samples were carried out using UV–visible spectrophotometer model (Labtronic LT 2900). It measures the percentage of radiation in the different regions such as ultra-violet (200–400 nm), visible (400–800 nm) and near IR (800–1200 nm) regions that is absorbed at each wavelength within ultra-violet, visible regions and near IR regions. The value of the direct band gap was calculated by using the given relation as:

$$E = \frac{hc}{\lambda}, \tag{2}$$

where h is the Plank's constant, c the speed of light and λ the wavelength.

2.6 *Drilling test*

Two small pieces have been cut from the bulk glass samples G1 and G2 with the help of diamond cutter of the size of $11 \times 9 \times 3$ mm. For the drilling test of the glass samples G1 and G2 are heat-treated at 1100°C for 3 h soaking time to convert into the glass ceramics.

3. Results and discussion

3.1 *XRD analysis*

The XRD patterns of all the glass samples are shown in figure 1 of glass compositions G1, G2, G3, G4 and G5, respectively. All the XRD patterns depict a broad diffuse scattering at different angles instead of sharp crystalline peaks, confirming a long range structural disorder characteristic of amorphous network. It is also observed that the XRD patterns of all the glass samples are almost similar and confirm the pure amorphous nature of the prepared glass samples.

3.2 *Density analysis of glass samples*

The density of the glasses (table 1) increased with addition of La₂O₃ due to its high density in comparison with other constituents of the glasses [18]. The values of density of the prepared glasses lie in the range from 2.104–3.061 g cc⁻¹. It is observed that the density of the glass samples G1, G2, G3, G4 and G5 are found to be increased with increasing doping concentration of lanthanum oxide which is due to the very high value of density of La₂O₃ (6.51 g cc⁻¹) in comparison to other used oxides and it is also due to the decreasing content of SiO₂ (2.65 g cc⁻¹). A similar trend in molar
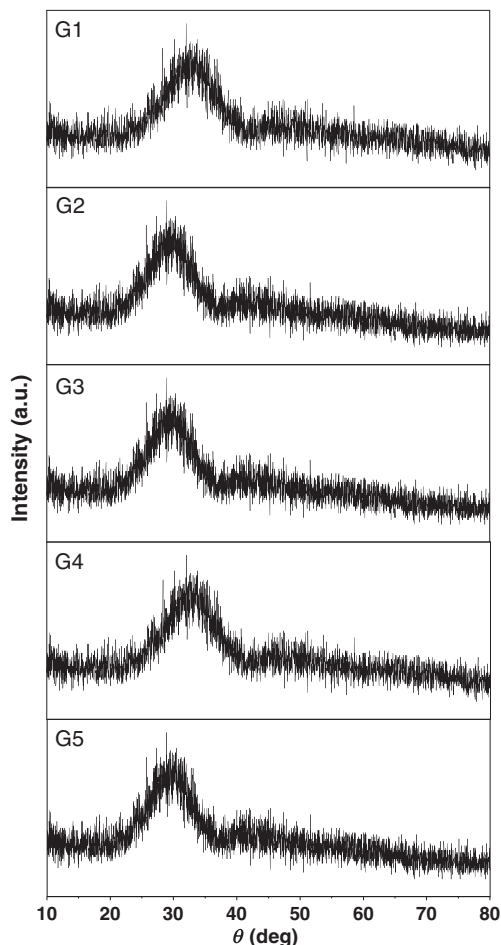

Figure 1. XRD patterns of G1, G2, G3, G4 and G5 glass samples.

volume (MV) was also observed with increasing La₂O₃ in the glasses. The MV of the glasses increases due to an increase in bond length or inter atomic spacing. In the present scenario, such an increase is due to the greater ionic radius of La (0.1061 nm) in comparison to the ionic radii of other glass constitutes [19] ($Si^{4+} = 0.026$ nm; $Al^{3+} = 0.039$ nm; $Mg^{2+} = 0.058$ nm; $Ca^{2+} = 0.100$ nm). Therefore, the volume corresponding to the structural unit with its surrounding space, V_m, is expected to increase by inserting a heavy metal oxide like La₂O₃. The density and increasing concentration of La₂O₃ are in good agreement with the results reported by Gautam *et al* [20].

3.3 *Fourier transform infrared spectroscopic study of glasses*

The Fourier transform infrared absorption spectra of annealed glass samples G1, G2, G3, G4 and G5 are shown in figures 2 and 3, respectively. FT-IR absorption peaks are very broad and sharp in nature towards the lower as well as higher wavelength side in the patterns of the glass samples. The observed absorption peaks have been numbered as 1, 2, . . . , 4 starting from higher wavenumber side to lower
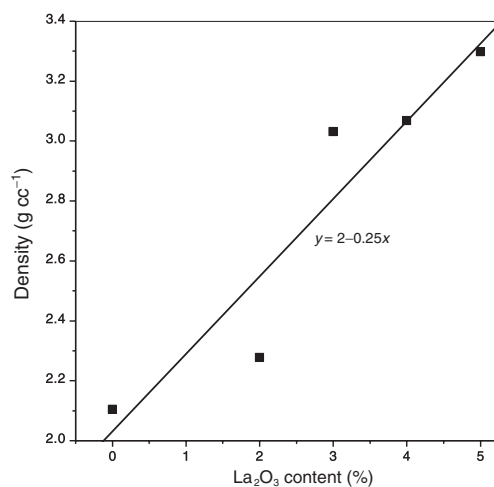
Figure 2. Variation of density *vs.* La$_2$O$_3$ content.

wavenumber side. The vibration types and IR absorption peaks of glasses G1, G2, G3, G4 and G5 are summarized in table 1. All annealed glasses showed four main absorption bands in the wavenumber region from 638 to 1631 cm^{-1} which are related to different types of the vibrations. Two broad bands were observed with lower wavenumber side at 759 and 644 cm^{-1}, indicate the general disorder in the silicate network, mainly due to the wide distribution of Q^n units (polymerization in the glass structure, where n denotes the number of bridging oxygens) occurring in the glasses [21]. In the IR spectra of these glasses, the band at 759 cm^{-1} has been also attributed to the vibrations of Si–O–Si groups with major movement of the silicon ions [22]. Aluminium containing crystalline silicates and aluminates show a band at 760 cm^{-1} corresponding to the stretching vibrations of the A1–O bond with aluminium in four-fold coordination [23]. The peak no. 4 at 645 cm^{-1} attributed to asymmetric stretching vibrations of Al–O–Al bond of octahedral [AlO$_6$] units of Al$_2$O$_3$ molecules [24,25]. The most intense broad band towards the low wavenumber side, 1200 cm^{-1}, represents the distribution of stretching vibrations in the SiO$_4$ tetrahedron with different numbers of bridging oxygen atoms with the centre of gravity fixed at $\sim$697 cm^{-1} (centre of the peaks 3 and 4) while the band in the 500–700 cm^{-1} region corresponds to bending vibrations of Si–O–Si and Si–O–Al linkages [26]. In case of aluminium coordination in the glass structure, the presence of an absorbance band of medium towards strong intensity in the 650–750 cm^{-1} region with the centre of gravity at $\sim$697 cm^{-1} is a typical feature for peralkaline glasses, and implies the tetrahedral coordination of Al [27]. Background noises were observed in all FT-IR spectra of the glass samples in the region from 3200 to 4000 cm^{-1}. It is also observed from the FT-IR spectra of the all glass samples that lower wavenumber side was more effective rather than high wavenumber side. Very intense and broad bands are present in the FT-IR spectra which indicate the good signature of the formation of glassy network.
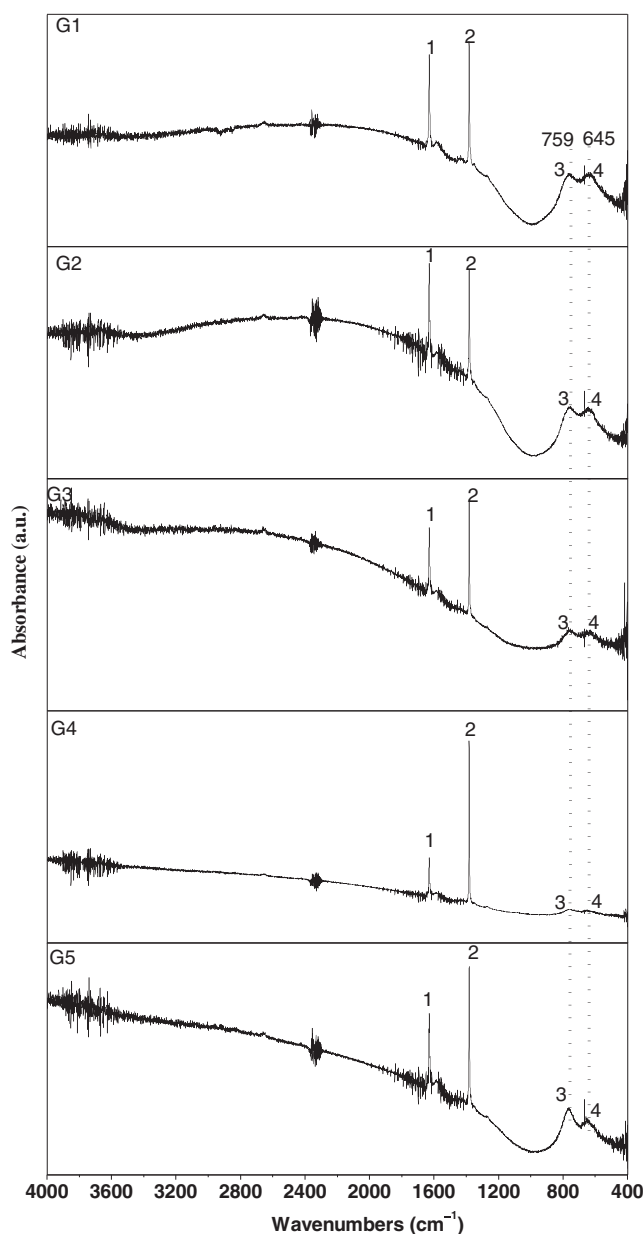

**Figure 3.** FT-IR spectra of different glass samples: G1, G2, G3, G4 and G5.

3.4 *UV–Vis spectroscopy*

UV–visible absorption spectra of various glass samples G1, G2, G3, G4 and G5 are shown in figure 4. There is only a sharp increase in absorption at energies close to the band gap that manifests itself as an absorption edge in the UV–visible absorption spectra of all the glass samples which guarantees the amorphous nature of glass samples. Generally, the absorption edge of the glass samples is determined by the strength of the oxygen bonding in the glass network. The changes in oxygen bonding in the glass network will change the characteristics of the absorption edge. As the material absorbs a photon of incident light, an electron is excited to a higher energy level [28]. Only a single transition

occurs in the wavelength region from 310 to 376 nm which is represented by two dotted parallel lines in all UV–Vis spectra [29]. The calculated values of optical band using equation (2) are listed in table 1. It is found that absorption edge intensity is increasing with decreasing content of the La_2O_3. It is observed from table 1 that the values of optical band gap initially increases with decreasing the amount of SiO_2, MgO and La_2O_3, respectively. This is due to the lower value of the band gap for lanthanum oxide (4.3 eV) in comparison with the above oxides. This shows the composition dependence of optical band gap of the synthesized glass samples.
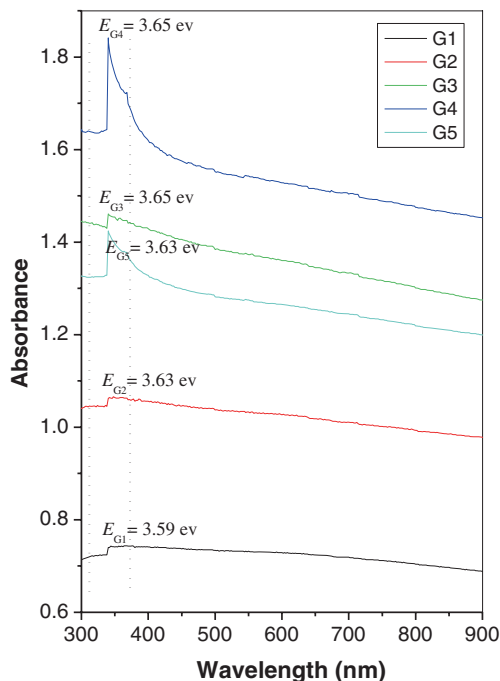
Figure 4. UV–Vis spectra of G1, G2, G3, G4 and G5 glass samples.
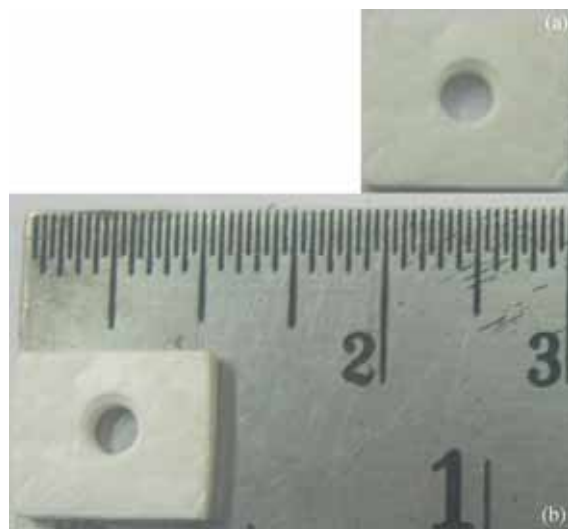
Figure 5. Photograph of drilling test for (**a**) GC1 and (**b**) GC2 specimens heated at 1100°C for 3 h.

3.5 *Mechanical behaviour*

The machined samples are shown in figure 5a and b. The rectangular shaped sample was cut using a diamond cutter before the machinability test. The glass ceramic samples GC1 and GC2, which are derived from their parent glass samples G1 and G2 showed excellent machinability, and a 3 mm thick hole was drilled successfully and completely. According to the results, the appropriate machining performance was obtained by using conventional heat treatment procedure without cracking the samples and confirm the very good machinability [30,31].

4. Conclusion

Bulk transparent glasses were prepared successfully in the glass SiO_2–Al_2O_3–MgO–K_2CO_3–CaO–MgF_2–La_2O_3 system. XRD analysis confirms the amorphous nature of the glasses. The density and the molar volume of the glasses increased as the La_2O_3 content increased. The increase in the density of the glass is due to the heavier lanthanum atomic weight compared with the other elements in the glass system. The increase in the molar volume of the glass is due to the increase in bond length or inter atomic spacing. FT-IR spectra show the formation of broad bands towards lower wavenumber side indicating these glasses are more effective and informative with respect to the lower wavenumber side. Stretching vibrations occur in the wavenumber range 850–990 cm^{-1} due to SiO_4 tetrahedron with different numbers of bridging oxygen atoms, while the band in the region 500–700 cm^{-1} corresponds to bending vibrations of Si–O–Si and Si–O–Al linkages. Optical band gap value lies in the range from 3.59 to 3.65 eV. Significant change was not observed in the value of optical band gap which shows the chemical stability of the prepared glasses. The produced glass ceramics exhibited excellent performance in machinability tests. These tests were carried out on both GC1 and GC2 samples without cracking or deformation.

References

[1] Merzbacher C I and White W B 1991 *J. Non-Cryst. Sol.* **130** 18

[2] Beal G H, Montierth M R and Smith G P 1972 *Tonind. Ztg. Keram.* **95** 351

[3] Grossman D G 1972 *J. Am. Ceram. Soc.* **55** 446

[4] Yu L, Xiao H and Cheng Y 2008 *Ceram. Int.* **34** 63

[5] Saucedo E M, Perera Y M and Robles D 2012 *Ceram. Int.* **38** 3161

[6] Mallik A, Basumajumdar A, Kundu P and Maiti P K 2013 *Ceram. Int.* **39** 2551

[7] Hill R 1996 *J. Mater. Sci. Lett.* **15** 1122

[8] Elgayar I, Aliev A E, Boccaccini A R and Hill R G 2005 *J. Non-Cryst. Solids* **351** 173

[9] Gautam C R, Kumar D and Parkash O 2010 *Bull. Mater. Sci.* **33** 145

[10] Gautam C R, Kumar D, Singh P and Parkash O 2012 *ISRN Spect.* **2012** 1

[11] Gautam C R, Singh P, Kumar D and Parkash O 2013 *Bull. Mater. Sci.* **36** 461

[12] Boch P and Niepce J C (ed.) 2007 *Ceramic materials processes* in *Properties and Applications* (London: ISTE)

[13] Nassar A M, Hamzawy E M A, Hafez F M, El Dera S S and Russel C 2012 *Ceram. Int.* **38** 1921

[14] Tulyaganov D U, Agathopoulos S, Fernandes H R, Ventura J M and Ferreira J M F 2004 *J. Eur. Ceram. Soc.* **24** 3521

[15] Taruta S, Ichinose T, Yamaguchi T and Kitajima K 2006 *J. Non-Cryst. Solids* **352** 5556

[16] Hong Li, De-Qiang Y, Chang-Ren Z and Jun-Guo R 2006 *J. Mater. Sci.: Mater. Med.* **17** 1133

[17] Gautam C R, Madheshiya A and Mazumder R 2014 *J. Adv. Ceram.* **3** 194

[18] Gautam C R and Yadav A K 2013 *Opt. Photo. J.* **3** 1

[19] Reddy A A, Tulyaganov D U, Kapoor S, Goel A, Pascual M J, Khartona V V and Ferreira J M F 2012 *RSC Advances* **2** 10955

[20] Gautam C R, Yadav A K, Mishra V K and Vikram K 2012 *Open J. Inor. Non-Meta. Mater.* **2** 47

[21] Tarte P 1967 *Spectrochim. Acta* **23** 2127

[22] Jellyman P E and Procter J P 1955 *J. Soc. Glass Tech.* **39** 173

[23] Kolesova V A 1960 *The structure of glass* (Translated from Russian) (New York: Consultant Bureau) vol 2, p 177

[24] Motke S G, Yawale S P and Yawale S S 2002 *Bull. Mater. Sci.* **25** 75

[25] Burdick V L and Day D E 1967 *J. Am. Ceram. Soc.* **50** 97

[26] Sharma S K, Yoder Jr H S and Matson D W 1988 *Geochim. Cosmochim. Acta* **52** 1961

[27] Pascual M J, Duran A and Prado M O 2005 *Phys. Chem. Glass* **46** 512

[28] Zaid M H M, Matori K A, Aziz S H A, Zakaria A and Ghazali M S M 2012 *Int. J. Mol. Sci.* **13** 7550

[29] Ghasemzadeh M, Nemati A, Hamnabard Z, Baghshahi S and Nozad G A 2012 *Synt. React. Inorg., Metal-Org. Nano-Metal. Chem.* **42** 958

[30] Ghasemzadeh M and Nemati A 2012 *Bull. Mater. Sci.* **35** 853

[31] Ercenk E and Yilmaz S 2015 *J. Ceram. Proc. Res.* **16** 169